

Effect of Increasing Concentrations on Sprayed $\text{Cu}_2\text{ZnSnS}_4$ Thin Films

N. Sebaa¹, M. Adnane¹, A. Djelloul^{1,3,*}, A. Abderrahmane^{1,2}, T. Sahraoui¹

¹ *Département de Technologie des Matériaux, Faculté de Physique, Université des Sciences et de la Technologie d'Oran Mohamed Boudiaf USTO-MB, BP 1505, El M'naouer, 31000 Oran, Algérie*

² *Centre de développement des technologies avancées (CDTA), cité 20 Aout 1956 Baba Hassen, Alger, Algérie*

³ *Centre de Recherche en Technologie des Semi-Conducteurs pour l'Energétique 'CRTSE' 02 Bd Frantz Fanon, BP: 140, 7 Merveilles, Alger, Algérie*

(Received 23 June 2019; revised manuscript received 20 October 2019; published online 25 October 2019)

Spray pyrolysis is a simple and low cost technique used for large thin films fabrication. In this paper, we reported the preparation of $\text{Cu}_2\text{ZnSnS}_4$ (CZTS) thin films with spray pyrolysis on glass substrates using different aqueous solutions. So, we chose to vary anions (S) and cations (Cu, Zn, Sn) concentrations. The purpose of this choice is the EDX analysis so that the percentage of copper is closer to 25 %; on the other hand, zinc and tin are around 12.5 % and sulfur at 50 %. The structural, chemical composition, morphological and optical properties of CZTS thin films were investigated using X-ray diffraction (XRD) and Raman spectroscopy, energy dispersive X-ray analysis (EDAX), scanning electron microscopy (SEM) and atomic force microscopy (AFM), and UV-visible spectroscopy analysis, respectively. The X-ray diffraction showed the formation of kesterite structure with dominant peaks along (112), (220) and (312) directions. Raman spectroscopy confirmed the existence of internal compressive stress in the CZTS thin films. The EDX analysis showed a better stoichiometry when optimizing the precursor concentrations. CZTS thin films showed low optical transmission and optical absorbance higher than $5 \times 10^4 \text{ cm}^{-1}$, which make the CZTS thin films prepared by spray pyrolysis technique suitable for CZTS solar cells.

Keywords: $\text{Cu}_2\text{ZnSnS}_4$, Spray pyrolysis deposition, XRD, UV-visible, AFM, Raman.

DOI: [10.21272/jnep.11\(5\).05009](https://doi.org/10.21272/jnep.11(5).05009)

PACS numbers: 61.46; 81.15.Rs; 61.05.Cp; 78.66.–Hf; 68.37.Ps; 33.20.Fb

1. INTRODUCTION

$\text{Cu}(\text{In}, \text{Ga})\text{Se}$ and CdTe based solar cells have high efficiency [1]. However, the use of Indium and Telluride in these kinds of solar cells make them very expensive. In addition, cadmium Cd and selenium Se on the other side are toxic; making CIGS and CdTe based solar cells unsuitable for practical application. CZTS is a p-type semiconductor with direct band gap energy in the range of 1.4 to 1.5 eV, its optical absorption coefficient is in the order of 10^4 cm^{-1} [2-4]. The optical and the electrical properties of CZTS, as well as the abundance of its composites in nature and their non-toxic behavior make this material more suitable than CIGS and CdTe . Moreover, CZTS based solar cells show efficiency of 8.6 % [5]. CZTS thin films have been synthesized using various techniques such as sol-gel technique [6], sputtering [7], spray pyrolysis [8], SILAR [9], electrodeposition [10], or deposition based on nanoparticle solutions [11].

Spray pyrolysis is simple, non-expensive technique appropriate for large-area semiconductors and metal oxides deposition. This technique is suitable for CZTS thin films deposition used in solar cell fabrication [12]; however, the stoichiometry of the CZTS thin films is very sensitive and highly depends on the precursor concentrations. In this work, we reported on the elaboration of CZTS thin films by spray pyrolysis on glass substrate. We discussed the effect of precursor concentrations on the chemical composition, structural and optical properties of CZTS thin films.

2. EXPERIMENTAL DETAILS

2.1 Materials and Methods

CZTS films were deposited on glass substrates at different concentrations of the cupric chloride ($\text{CuCl}_2, 2\text{H}_2\text{O}$), zinc chloride ($\text{ZnCl}_2, \text{H}_2\text{O}$) and thiourea $\text{SC}(\text{NH}_2)_2$ purchased from BIOCHEM Chemopharma, and stannic chloride ($\text{SnCl}_4, 2\text{H}_2\text{O}$) from Cheminova. We dissolved the precursors in a mixture of ethanol and acetone, the experimental parameters are shown in Table 1. In our experiment, we used excess of thiourea to compensate the loss of sulfur during the heating process [13, 14]. The deposition time was 2 min and the distance from nozzle to substrate was fixed at 40 cm, the substrate temperature was chosen as 300 °C during the experiment. We used microscope slides ($25.4 \times 76.2 \text{ mm} \times 1.0 \text{ mm}$) substrates that were ultrasonically cleaned in acetone, ethanol and distilled water for 5 min in each beaker and followed by drying under nitrogen gas. During our experimental approach, we adjusted the stoichiometry of two samples of CZTS by simultaneously varying the concentrations of the anions (S) and cations (Cu, Zn, Sn). For this reason, we obtained two S1 and S2 samples. For the first S1, we opted for the following concentrations: $[\text{S}^{2-}] = 8[\text{Cu}^{2+}]$; $[\text{Cu}^{2+}] = 2[\text{Zn}^{2+}] = 2[\text{Sn}^{2+}]$; for the second S2: we obtained $[\text{S}^{2-}] = 6[\text{Cu}^{2+}]$; $[\text{Cu}^{2+}] = 2[\text{Zn}^{2+}]$; $[\text{Cu}^{2+}] = 2.5[\text{Sn}^{2+}]$.

These concentrations were optimized by decreasing the report $[\text{S}^{2-}]/[\text{Cu}^{2+}]$ slightly and increasing the $[\text{Cu}^{2+}]/[\text{Sn}^{2+}]$ ratio to move closer to the stoichiometry of CZTS.

In this experiment, we discussed the formation of

* djelloulcrtse@gmail.com,
nadia.sebaa@univ-usto.dz

CZTS thin films during pyrolysis under the same parameters such as the temperature and deposition time. Thickness of layers was measured by the profilometer (BRUKER DEKTAK XT), X-ray diffractometer (Panalytical DY 1352) and Raman spectrometer (jobin yvon HORIBA) recorded for the purpose of examining the crystal, the morphology of the surface was observed by scanning electron microscope SEM (JEOL JSM-6610LA) and AFM (JSPM-5200), the elemental composition was determined by dispersive energy spectrometer (EDS) REF equipment, and the optical properties were examined using UV-VIS spectrophotometer (Perkin Elmer lambda 20) in the range 250-1200 nm.

Table 1 – CZTS thin film deposition parameters

Samples	[Cu]	[Zn]	[Sn]	[S]
Sample 1	0.01 M	0.005 M	0.005 M	0.08 M
Sample 2	0.02 M	0.01 M	0.008 M	0.12 M

3. RESULTS AND DISCUSSION

3.1 Thickness Measurement

Fig. 1 shows the obtained CZTS thin films. Thickness values of CZTS films are approximately 372 nm for sample 1 and 930 nm for sample 2. CZTS thin films at both thicknesses were uniform and the color changed from grayish black to dark black with increasing film thickness, which means that high concentrations played a role in the rapid growth of layers.

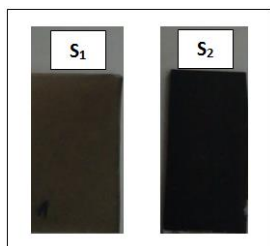


Fig. 1 – Photographs of synthesized CZTS thin films

3.2 Structural Analysis

XRD patterns of CZTS thin films prepared are shown in Fig. 2, the synthesized films are of polycrystalline type with an intense peak located at the position corresponding to the preferential direction (112) which is characteristic of a kesterite structure. The major peaks located at the positions corresponding to the directions (112), (220), and (312) respectively indicate a good crystallinity of the compounds [15, 16], the preferred orientation (112) was observed for all deposited films, sample S1 expectedly shows a lower peak intensity in comparison to sample S2 and the crystallite size D in sample 2 is double compared to sample 1. This is probably due to the existence of a high concentration of copper atoms in sample 1, for this reason the excess of copper induces the increase of the thickness. All diffraction peaks for both CZTS films correspond to the tetragonal CZTS structure (JCPDS card no. 26-0575). The crystallite size is about 49, 102 Å for samples S1 and S2. The lattice parameters and D of CZTS thin films are summarized in Table 2. The crystallite size is small because of the absence of treatment at higher temperatures and sulfurization [17].

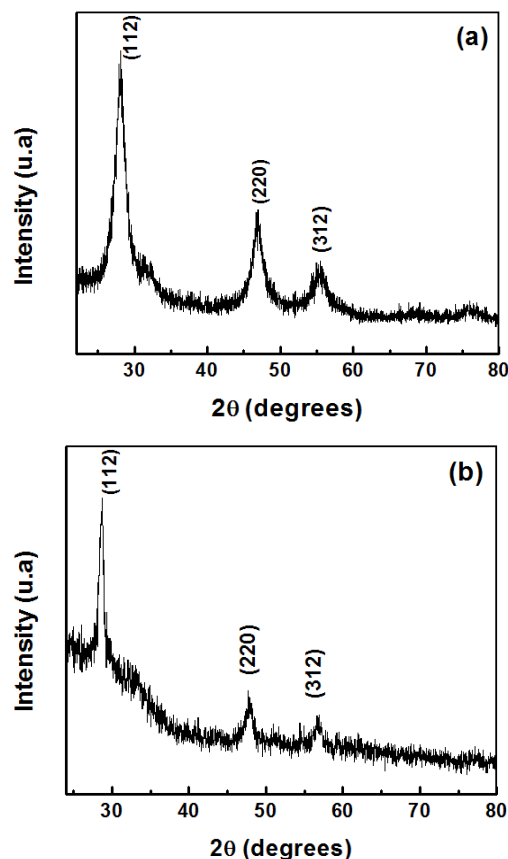


Fig. 2 – XRD pattern of the samples: S1 (a) and S2 (b)

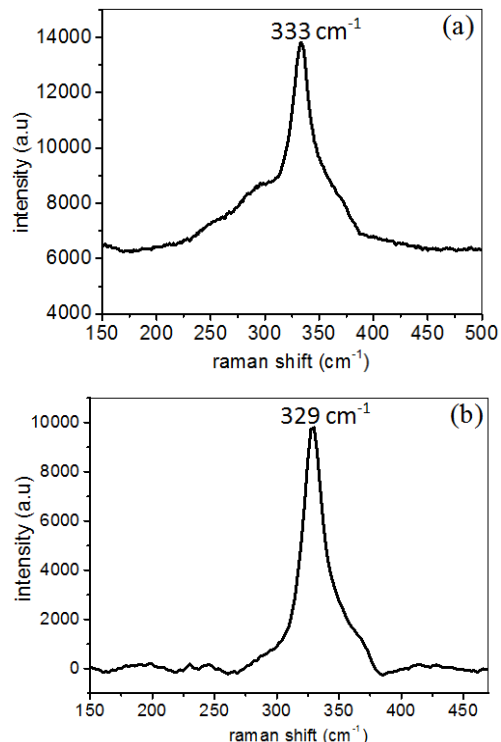


Fig. 3 – Raman spectra of the samples: S1 (a) and S2 (b)

The kesterite phase of CZTS is also verified by Raman spectroscopy, which is presented in Fig. 3. Raman spectrum was changed with changing concentrations, a single intense peak was observed at 329 cm^{-1} and at

333 cm^{-1} for sample S1 and sample S2 respectively that is attributed to the characteristic Raman peak of CZTS according to the value reported for CZTS by L. Sun et al. [18] and B. Flynn [19] compared to other literatures, the dominant peak is around 338 cm^{-1} [20]. This displacement towards the low wave number direction may be due to the existence of internal compressive stress in CZTS thin films produced without annealing under sulfur atmosphere [21]. Raman results show that there are no additional peaks of other phases presented in different studies [22, 23].

Table 2 – Lattice parameters and crystallite size of CZTS thin films

Sample	Lattice Constant $a, \text{\AA}$	Lattice Constant $c, \text{\AA}$	Crystallite size $D, \text{\AA}$
S1	5.48	11.21	49
S2	5.48	10.54	102

3.3 Morphological Properties

EDAX spectrum of CZTS layers with different concentrations are shown in Fig. 4, where peaks of copper, zinc, tin and sulfur are clearly observed, that indicates the presence of the four compounds for both samples, and also the peaks due to silicon and oxygen have been observed that came from substrate. Atomic percentage of the samples is presented in Table 3, theoretically, expected stoichiometric composition of CZTS (in terms of at. %) is Cu:Zn:Sn:S equal to 25.00:12.50:12.50:50.00 [20], we observed a difference concerning the stoichiometry of sample S1, it has the large stoichiometry deviation $\text{Cu}_{3.49}\text{Sn}_{3.09}\text{Zn}_1\text{S}_{5.37}$ when we consider zinc is one. But the second has the best stoichiometry deviation $\text{Cu}_{2.55}\text{Sn}_1\text{Zn}_{1.35}\text{S}_{4.39}$ when we choose tin is one.

In Fig. 5, we can see SEM images of CZTS thin films which show grains uniformly distributed and covering the substrate surface. In sample S2, the grain structure

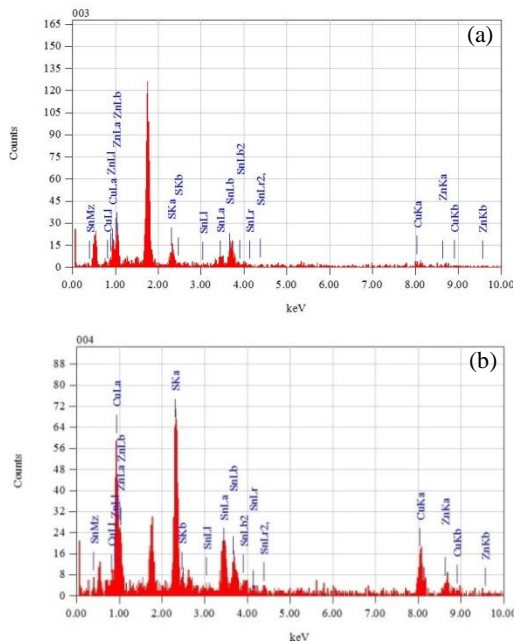


Fig. 4 – EDAX spectrum of the samples: S1 (a) and S2 (b)

Table 3 – Chemical compositions of different CZTS thin films

Sample name	Elemental composition (in at. %)			
	Cu	Zn	Sn	S
S1	26.92	7.72	23.86	41.49
S2	27.46	14.52	10.77	47.25

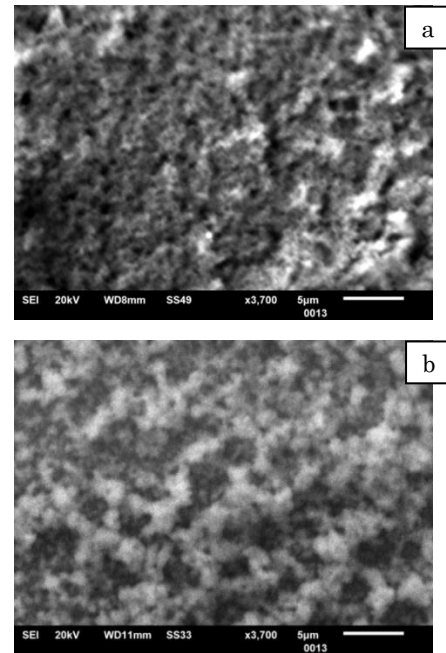


Fig. 5 – SEM micrograph of the samples: S1 (a) and S2 (b)

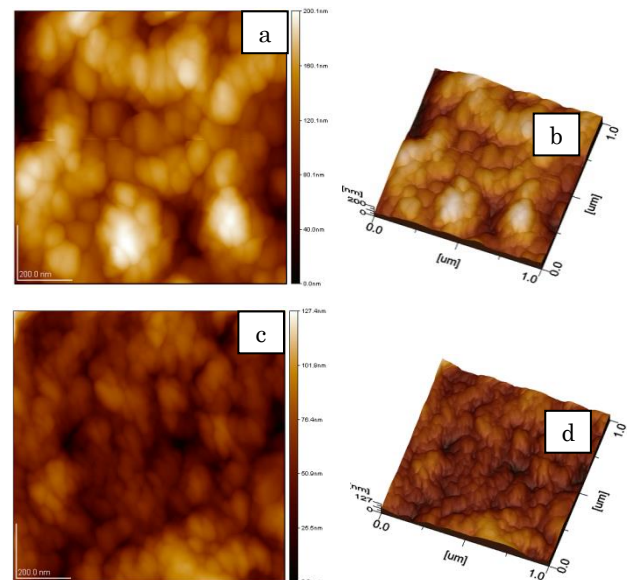


Fig. 6 – The AFM images of the samples: topographical 2D and 3D of the sample S1 (a, b); topographical 2D and 3D of the sample S2 (c, d)

is more densely packed than in sample S1; this indicates that grain growth is improved due to the increase in thickness. The corresponding AFM images of CZTS film are shown in Fig. 6, the surface height fluctuations are detected by line scan by AFM system, the average

surface height fluctuation of samples S1 and S2 is about 200 and 127 nm respectively, the root mean square (R_{ms}) roughness of samples S1 and S2 is 30 and 13 nm respectively. Moreover, the CZTS thin films appear smooth and are formed of densely packed and uniform spheres.

3.4 Optical Properties

The optical spectra of the synthesized films were obtained by the measurements of transmission and absorption as can be seen in Fig. 7. CZTS thin films deposited by pyrolysis spray have a low transmission in the visible portion of the wavelengths around 35 % and 12 % for the samples S1 and S2 respectively (Fig. 7a). Absorption coefficients calculated from the transmission data are around 5.10^4 cm^{-1} (Fig. 7b). It can be noticed that the value of absorption coefficients increases with increasing concentrations and also with increasing thickness.

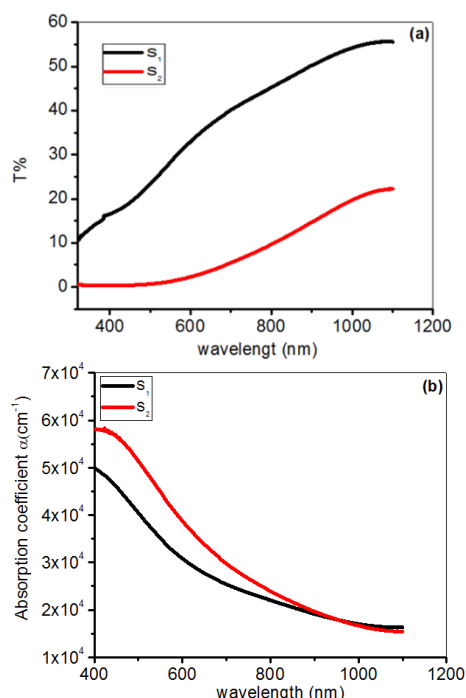


Fig. 7 – Transmittance (a); absorption coefficient (b) of CZTS thin films synthesized with different concentrations

REFERENCES

- Philip Jackson, Roland Wuerz, Dimitrios Hariskos, Erwin Lotter, Wolfram Witte, Michael Powalla, *Phys. Status Solidi RRL*, **1** (2016).
- S. Hemalatha, J. Tamil Illakkiya, R. Oommen, P. Usha, R. Lakshmi, *Int. J. ChemTech Res.* **6**, 1994-1997 (2014).
- S. Kermadi, S. Sali, F. Ait Ameer, L. Zougar, M. Boumaour, A. Toumiat, N.N. Melnik, D.W. Hewak, Anca Duta, *Mater. Chem. Phys.* **1** (2015).
- T. Srinivasa Reddy, R. Amiruddin, M.C. Santhosh Kumar, *Sol. Energy Mater. Sol. Cells* **143**, 128 (2015).
- G. Larramona, S. Bourdais, A. Jacob, C. Choné, T. Muto, Y. Cuccaro, B. Delatouche, C. Moisan, D. Péré, G. Dennler, *J. Phys. Chem. Lett.* **5**, 3763 (2014).
- N. Moritake, Y. Fukui, M. Oonuki, K. ko Tanaka, H. Uchiki,

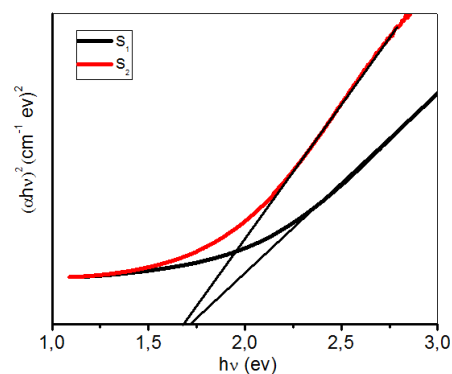


Fig. 8 – Band gap variations of CZTS thin films synthesized with different concentrations

In order to obtain the optical band gap of the films, the linear part of the spectrum is extrapolated to zero as shown in Fig. 8; we found that the band gap decreases from 1.72 to 1.68 eV with increasing concentrations which is in good agreement with CZTS band gap values reported by other authors [24]. The observed band gap values are little higher than the reported experimental as well as theoretical value of CZTS thin films (1.45 to 1.6 eV) [25, 26]. The high value gap for as-deposited thin films may be attributed to residual organic compound precursor and low grain size [27]. However, the band gap values of our samples are favorable for CZTS solar cells.

4. CONCLUSIONS

In conclusions, we successfully prepared $\text{Cu}_2\text{ZnSnS}_4$ thin films by spray pyrolysis. X-ray diffraction and Raman spectroscopy showed that the obtained CZTS thin films are polycrystalline with kesterite structure and with the absence of other second phase compounds. The CZTS thin films were almost stoichiometric with crystallite sizes of 49 to 102 Å. The band gap of CZTS thin films varied between 1.68 and 1.72 eV, and optical absorbance was higher than $5 \times 10^4 \text{ cm}^{-1}$ that make this material suitable for CZTS solar cells.

ACKNOWLEDGEMENTS

The authors thank the help from Dr. Zerdali Mokhtar, professor in USTO-MB for the high quality AFM image acquisitions and analysis.

Phys Status Solidi C **6**, 1233 (2009).

- B.G. Mendis, M.D. Shannon, M.C.J. Goodman, J.D. Major, R. Claridge, D.P. Halliday, K. Durose, *Prog. Photovolt: Res. Appl.* **22**, 24 (2014).
- Z. Seboui, A. Gassoumi, N. Kamoun-Turki, *Mater. Sci. Semicond. Proc.* **26**, 360 (2014).
- S. Ma, J. Sui, L. Cao, Y. Li, H. Dong, Q. Zhang, L. Dong, *Appl. Surf. Sci.* **349**, 430 (2015).
- Y. Lin, S. Ikeda, W. Septina, Y. Kawasaki, T. Harada, M. Matsumura, *Sol Energy Mater. Sol. Cells* **120**, 218 (2014)
- M. Zhou, Y. Gong, J. Xu, G. Fang, Q. Xu, J. Dong, *J. Alloys Compd.* **574**, 272 (2013).
- H. Cui, X. Liu, L. Sun, F. Liu, C. Yan and X. Hao, *Coatings* **7**, 19 (2017).

13. Z. Seboui, Y. Cuminal, N. Kamoun-Turki, *J. Renewable Sustainable Energy* **5**, 023113 (2013).
14. Y. Larbah, M. Adnane, T. Sahraoui, *Mater. Sci. Poland* **33**, 491 (2015).
15. Z. Seboui, A. Gassoumi, Y. Cuminal, N. Kamoun-Turki, *Superlatt. Microstr.* **75**, 586-592 (2014).
16. U. Chalapathi, S. Uthanna, V.S. Raja, *Sol. Energy Mater. Sol. Cells* **132**, 476 (2015).
17. M. Valdes, G. Santoro, M. Vazquez, *J. Alloys Compd.* **585**, 776 (2014).
18. L. Sun, J. He, H. Kong, F. Yue, P. Yang, J. Chu, *Sol. Energy Mater. Sol. Cells* **95**, 2907 (2011).
19. B. Flynn, W. Wang, C.H. Chang, and G.S. Herman, *Phys. Status Solidi A* **209**, 2186 (2012)
20. A.G. Kannana, T.E. Manjulavallia, J. Chandrasekaran, *Procedia Eng.* **141**, 15 (2016)
21. H. Yoo, J.H. Kim, *Sol Energy Mater. Sol. Cells* **95**, 239 (2011).
22. S. Thiruvenkadam, D. Jovina, A. Leo Rajesh, *Sol. Energy* **106**, 166 (2014).
23. M.E. Rodriguez, M. Placidi, O.V. Galán, V.I. Roca, X. Fontané, A. Fairbrother, D. Sylla, E. Saucedo, A.P. Rodríguez, *Thin Solid Films* **535**, 67 (2013).
24. Z. Seboui, Y. Cuminal, and N.K. Turki, *J. Renewable Sustainable Energy* **5**, 023113 (2013).
25. M. Valdes, G. Santoro, M. Vazquez, *J. Alloys Compd.* **585**, 776 (2014)
26. J. Zhi, W. Shurong, L. Zhishan, Y. Min, L. Sijia, L. Yilei, Z. Qichen, H. Ruiting, *Mater. Sci. Semicond. Proc.* **57**, 239-243 (2017).
27. A.El kissani, A. Ammar, L. Nkhaili, K. El assali, A. Outzourhit, *EU PVSEC* **31** (2015).

Вплив збільшення концентрацій при отриманні тонкої плівки $\text{Cu}_2\text{ZnSnS}_4$

N. Sebaa¹, M. Adnane¹, A. Djelloul^{1,3}, A. Abderrahmane^{1,2}, T. Sahraoui¹

¹ *Département de Technologie des Matériaux, Faculté de Physique, Université des Sciences et de la Technologie d'Oran Mohamed Boudiaf USTO-MB, BP 1505, El M'naouer, 31000 Oran, Algérie*

² *Centre de développement des technologies avancées (CDTA), cité 20 Aout 1956 Baba Hassen, Alger, Algérie*

³ *Centre de Recherche en Technologie des Semi-Conducteurs pour l'Energétique 'CRTSE' 02 Bd Frantz Fanon, BP: 140, 7 Merveilles, Alger, Algérie*

Спрей-піроліз – це проста техніка, що використовується для виробництва великих тонких плівок. У роботі ми повідомляємо про виготовлення тонких плівок $\text{Cu}_2\text{ZnSnS}_4$ (CZTS) методом спрей-піролізу на скляних підкладках з використанням різних водних розчинів. Отже, ми вирішили змінювати концентрації аніонів (S) та катіонів (Cu, Zn, Sn). Метою цього вибору є аналіз EDX, щоб відсоток міді був ближче до 25 %; з іншого боку, цинк і олово складають близько 12.5 %, а сірка – 50 %. Структурний та хімічний склад, морфологічні та оптичні властивості тонких плівок CZTS досліджували за допомогою рентгенівської дифракції (XRD) та Раманівської спектроскопії, енергетично-дисперсійного рентгенівського аналізу (EDAX), скануючої електронної мікроскопії (SEM) та атомно-силової мікроскопії (AFM) та спектроскопічного аналізу в ультрафіолетовому та видимому діапазонах відповідно. Рентгенівська дифракція показала утворення кестеритової структури з домінуючими піками в напрямках (112), (220) та (312). Раманівська спектроскопія підтвердила наявність внутрішньої напруги стиску в тонких плівках CZTS. Аналіз EDX показав кращу стехіометрію при оптимізації концентрацій прекурсора. Тонкі плівки CZTS демонстрували низьку оптичну пропускну здатність та оптичне поглинання вище $5 \times 10^4 \text{ cm}^{-1}$, завдяки чому тонкі плівки CZTS, підготовлені методом спрей-піролізу, підходять для сонячних батарей CZTS.

Ключові слова: $\text{Cu}_2\text{ZnSnS}_4$, Осадження методом спрей-піролізу, Рентгенівська дифракція, Ультрафіолетовий та видимий діапазони, Атомно-силова мікроскопія, Раманівська спектроскопія.